Available online at ScienceDirect
ScienceDirect
J. Mater. Sci. Technol., 2014, 30(8), 835–838
www.JMST.org

Surface Passivation Performance of Atomic-Layer-Deposited Al_2O_3 on p-type Silicon Substrates

Yanghui Liu, Liqiang Zhu, Liqiang Guo, Hongliang Zhang, Hui Xiao*
Ningbo Institute of Materials Technology and Engineering, Chinese Academy of Sciences, Ningbo 315201, China

[Manuscript received July 29, 2013, in revised form August 20, 2013, Available online 19 December 2013]

Surface passivation performances of Al_2O_3 layers deposited on p-type Czochralski Si wafers by atomic layer deposition (ALD) were investigated as a function of post-deposition annealing conditions. The maximal minority carrier lifetime of ~4.7 ms was obtained for Al_2O_3 passivated p-type Si. Surface passivation mechanisms of Al_2O_3 layers were investigated in terms of interfacial state density (D_{it}) and negative fixed charge densities (Q_{fix}) through capacitance–voltage (C–V) characterization. High density of Q_{fix} and low density of D_{it} were needed for high passivation performances, while high density of D_{it} and low density of Q_{fix} degraded the passivation performances. A low D_{it} was a prerequisite to benefit from the strong field effect passivation induced by high density of negative fixed charges in the Al_2O_3 layer.

KEY WORDS: Atomic layer deposition; Al_2O_3; Passivation; Films

1. Introduction

The high cost of solar photovoltaic (PV) panels is a major deterrence to the market penetration of the technology. Therefore, it is highly desirable to improve the solar cells efficiency and reduce the thickness of the Si wafers in c-Si solar cells, which results in the decrease of the cost per watt. With the reduction of the thickness of crystalline silicon (c-Si) wafer, surface passivation is getting increasingly important. Conventionally, screen printed aluminum back surface field (Al-BSF) is applied to the c-Si solar cell flow[1]. However, Al-BSF only shows a moderate passivation quality with typical rear surface recombination velocities (S_{rear}) ranging from 200 to 1000 cm/s and a low internal reflectivity R_{back} of ~70%[2]. Optimization of the screen-printing steps with the reduced finger width and the improved Al-BSF would be the main approaches to improve the efficiency[3]. Since the excellent surface passivation is essential for high-efficiency solar cells, passivated emitter and rear locally diffused (PERL) or passivated emitter and rear cell (PERC) concepts have been proposed to get a high solar cell efficiency with dual Si surface being effectively passivated. A wide range of materials have been adopted for surface passivation applications, such as a-SiN_x[4], SiO_2[5], a-Si[6] and a-SiC_x[7]. A record efficiency of 25% has been realized on c-Si solar cells with a thermally grown SiO_2 passivated rear surface[5]. While in recent years, aluminum oxide (Al_2O_3) has attracted much attention as a next generation material for surface passivation. Thanks to a high density of negative fixed charges stored at the interface region, excellent field-effective passivation performances have been observed on both lightly and highly doped p- and n-type c-Si surfaces[8–11]. A high efficiency of 23.2% has been obtained by passivating front side boron emitter for n-type PERL cell[12,13]. At least two mechanisms would result in the improvements of the passivation performances[2,14], such as: (i) interfacial state density (D_{it}), (ii) field effect passivation, that is, a strong reduction of one type carrier by incorporating fixed charge (Q_{fix}) in the interface. As an effective method, an additional post-deposition annealing (PDA) is also required to activate the surface passivation after depositing Al_2O_3 on Si surface. The passivation mechanisms have been studied by optical second-harmonic generation (SHG), corona charging experiment, capacitance–voltage measurements and electron paramagnetic resonance, etc[15–17]. Though there are reports on the temperature-dependent passivation performance of Al_2O_3 thin films on c-Si surface, the detail passivation mechanisms of Al_2O_3 thin films are still required to be studied. In our previous work[11], both antireflectance and surface passivation performances were addressed for Al_2O_3 thin films, while the detailed reasons for surface passivation performances have not been discussed. In this work, effective minority carrier lifetime of the Al_2O_3 thin films passivated c-Si has been characterized. The passivation performances have been studied and have been correlated with negative fixed charges (Q_{fix}) and interfacial state density (D_{it}). The results indicate that the passivation performances of Al_2O_3 thin films depended greatly on D_{it} when Q_{fix} is high.

* Corresponding author. Assoc. Prof., Ph.D.; Tel.: +86 574 86686791; Fax: +86 574 86690355; E-mail address: lqzhu@nimte.ac.cn (L. Zhu).

http://dx.doi.org/10.1016/j.jmst.2013.12.005

2. Experimental

Boron-doped p-type Czochralski single crystalline silicon (c-Si) wafers (shiny-etched, (100)-oriented, 400 μm thick, 30 Ω cm, 15 cm in diameter) purchased from QL Electronics Corporation were used as the substrates. Before experiments, the wafers were cleaned using RCA method and followed by a diluted HF dip to remove the native oxide layer. Al_2O_3 thin films were deposited by using $Al(CH_3)_3$ (TMA) and water as precursors in a thermal atomic layer deposition (ALD) reactor (Lucida™ D200B, NCD Technology, Korea) at 200 °C with a 100 sccm background flow of N_2. A cycle of the reaction consisted of a 0.3 s injection of TMA vapor followed by 7 s N_2 purge and a 0.1 s injection of H_2O vapor followed by 7 s N_2 purge. The deposition rate is estimated to be around 0.125 nm/cycle. ALD process is based on sequential, self-limiting surface chemical "half-reactions"[18,19]. The surface chemistry during ALD Al_2O_3 can be described as:

$$AlOH^* + Al(CH_3)_3 \rightarrow AlOAl(CH_3)_2^* + CH_4 \quad (1)$$

$$AlCH_3^* + H_2O \rightarrow AlOH^* + CH_4 \quad (2)$$

where the asterisk designates the surface species. The main driving force for the efficient reactions is the formation of a very strong Al−O bond. Therefore, Al_2O_3 film thickness could be controlled accurately by controlling the number of reaction cycles. It should be noted here that there are some residual Al−OH* bonds during the reaction. O−H bonds would be easily broken, resulting in the interstitial H atoms within the Al_2O_3 matrix. Such H atoms play an important role in the passivation performance. In order to measure the effective minority carrier lifetime (τ_{eff}), clean c-Si wafers were coated by 30 nm Al_2O_3 films symmetrically as lifetime sample and were annealed at different temperatures in atmosphere ambient. These samples were characterized by microwave photoconductivity decay (μ-PCD) method taken by Semilab WT-2000PVN lifetime tester. The excess carriers were generated by a 200 ns laser pulse with a wavelength of 904 nm and a spot size of 1 mm^2. The maximum achieved minority carrier lifetime (τ_{eff}) was investigated. The minority carrier lifetime (τ_{eff}) depends on both bulk minority carrier lifetime (τ_{bulk}) and surface recombination velocity S_{eff}, shown as follows[20]:

$$\frac{1}{\tau_{eff}} = \frac{1}{\tau_{bulk}} + \frac{2S_{eff}}{W} \quad (3)$$

where W is the wafer thickness. When the bulk minority carrier lifetime is assumed to be infinite, the calculated S_{eff} value marks an upper limit to the effective surface recombination velocity.

Spectroscopic ellipsometry was employed to obtain the thickness of Al_2O_3 films on shiny-etched Si. For electrical measurements, copper electrodes were evaporated through shadow masks. Sputtered Al layer was used as the metal rear side contact of the metal-oxide-semiconductor (MOS) structure. Capacitance−voltage ($C-V$, 1.0 MHz) characterizations were performed by using a Keithley 4200 SCS semiconductor parameter analyzer.

3. Results and Discussion

To activate the passivation performance, a series of post-deposition annealing (PDA) at different temperatures for different times were carried out. Fig. 1 shows the effective minority carrier lifetime (τ_{eff}) and the surface recombination velocity (S_{eff}) of p-type c-Si wafers passivated by 30 nm Al_2O_3. For original c-Si wafer, the τ_{eff} was measured to be ∼6 μs and the S_{eff} was estimated to be ∼3200 cm/s (not shown in Fig. 1). After depositing a 30 nm-thick Al_2O_3 layers, a higher τ_{eff} of ∼900 μs is obtained, corresponding to a lower S_{eff} of ∼21 cm/s (not shown in Fig. 1). The results show that the effective minority carrier lifetime is improved when the Al_2O_3 thin films is deposited on c-Si surface. To study the full potential and the thermal stability of the surface passivation performances of Al_2O_3 layers, the lifetime samples were exposed to PDA at temperature (T_a) ranging from 300 to 600 °C with PDA time of 2 and 5 min. A flash annealing was also performed at 900 °C for 3 s. The annealed films affords a high level of surface passivation with $S_{eff} < 10$ cm/s for annealing temperature between 350 and 550 °C with annealing time of 2 and 5 min. Extremely low S_{eff} values are obtained at $T_a = 350$ °C, i.e., S_{eff} of ∼4.0 cm/s with τ_{eff} of 4.7 ms and ∼6.8 cm/s with τ_{eff} of 2.8 ms for PDA time of 5 and 2 min, respectively. Though, there is a decrease in τ_{eff} for PDA temperatures above 350 °C, it keeps high above 2 ms for PDA temperature below 550 °C. In addition, with PDA temperatures ranging between 300 and 550 °C, PDA treatments for 5 min result in the improved passivation performance as compared to PDA treatments for 2 min. Such improvements are due to the decreased D_{it} and the increased Q_{fix}. While for PDA temperature at 600 °C, the degraded passivation performance is observed for 5 min as compared to that for 2 min. The flash annealing at 900 °C for 3 s yields a moderate level of surface passivation performance with a S_{eff} of ∼160 cm/s ($\tau_{eff} = 120$ μs) (not shown in Fig. 1). Such passivation degradations are due to the deteriorated interface properties.

To investigate the underlying mechanisms for the Al_2O_3 passivation performances, we studied the electrical behaviors of the PDA treated Al_2O_3 films with $C-V$ characterizations at 1.0 MHz at room temperature. Fig. 2 shows the $C-V$ curves. Voltage was swept from −0.5−3 V, and then back. Taking the work function difference (Φ_{ms}) between copper electrode and Si substrate to be −0.5 eV, big positive shifts in $C-V$ curves are observed for all the samples. Such big positive shifts indicate the presence of negative Q_{fix} with high densities within Al_2O_3 thin films.

Q_{fix} in Al_2O_3 layer could be determined from flat-band voltage (V_{FB}) by using the following relationship[11]:

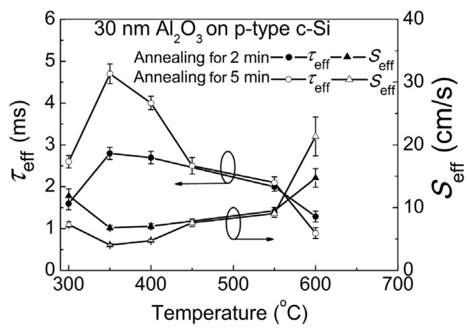

Fig. 1 Effective minority carrier lifetime (τ_{eff}) and effective surface recombination velocity (S_{eff}) for p-type Si passivated by 30 nm Al_2O_3 PDA treated at temperature (T_a) ranging from 300 to 600 °C with PDA time of 2 and 5 min.

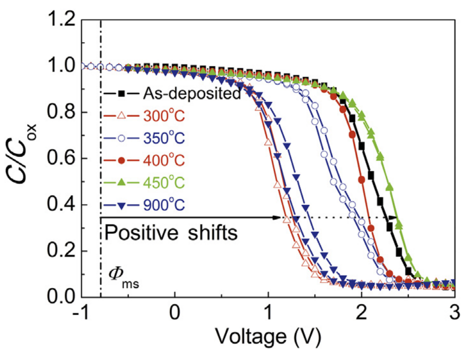

Fig. 2 Normalized $C-V$ curves of MOS structures with Al_2O_3 films on p-type Si substrates measured at 1.0 MHz: As-deposited, PDA at 300, 350, 400 and 450 °C for 5 min and flash annealed at 900 °C for 3 s.

$$Q_{fix} = \left(\frac{\Phi_{ms}}{q} - V_{FB}\right)\frac{\varepsilon_{Al_2O_3}\varepsilon_0}{d} \tag{4}$$

where Q_{fix}, q, d, $\varepsilon_{Al_2O_3}$ and ε_0 are the fixed charge density, elementary charge, thickness of Al_2O_3, dielectric constant of Al_2O_3 and permittivity of vacuum, respectively. D_{it} was estimated by Lehovec's method from the flat-band voltage condition of $C-V$ characteristics[21]:

$$D_{it} = \frac{(C_i - C_{FB})C_{FB}}{3\left|(\delta C/\delta V)_{FB}\right| \cdot q\kappa TA} - \frac{C_i^2}{(C_i - C_{FB})Aq^2} \tag{5}$$

where C_{FB}, $(\delta C/\delta V)_{FB}$ and C_i are the capacitance at flat-band voltage, the partial derivative of capacitance at flat-band voltage and the capacitance at the accumulate region, respectively.

Fig. 3 illustrates the Q_{fix} and D_{it} extracted from $C-V$ curves shown in Fig. 2. It could be seen from the figure that there is a high density of negative Q_{fix} in the order of $\sim 10^{12}$ cm^{-2}. In our case, Al_2O_3 thin films were deposited using $Al(CH_3)_3$ (TMA) and water as precursors. The reaction between TMA and water would result in the interstitial H atoms and Al–OH bonds within the Al_2O_3 matrix. Peacock and Robertson[22] indicated that interstitial H within Al_2O_3 would act as a deep trap site for electrons. Therefore, the existence of interstitial H in Al_2O_3 would result in the negative fixed charges within Al_2O_3. The maximum Q_{fix} is obtained for the 450 °C annealed sample with the value of about -5×10^{12} cm^{-2}, while the lowest Q_{fix} is obtained for the PDA sample at 300 °C with the value of about -3×10^{12} cm^{-2}. Though there are small changes in Q_{fix}, the big changes take place in effective minority carrier lifetime (τ_{eff}), as shown in Fig. 1. Therefore, the density of Q_{fix} will not determine the passivation performance when it arrives at the order of $\sim 10^{12}$ cm^{-2}. The D_{it} behaviors would explain the effective minority carrier lifetime (τ_{eff}) behaviors. It could be seen from Fig. 3 that there is a high density of D_{it} in the order of $\sim 10^{12}$ cm^{-2} eV^{-1}. For the as-deposited sample, though a high density of Q_{fix} exists, D_{it} is relatively high of $\sim 6.5 \times 10^{12}$ cm^{-2} eV^{-1}, which results in a low τ_{eff} of ~ 900 μs. While for PDA samples with PDA temperatures between 350 and 400 °C, a significant decrease in D_{it} to the value of $\sim 3 \times 10^{12}$ cm^{-2} eV^{-1} results in the improved passivation performance. At these temperatures, H atoms will be released from Al–OH bonds produced during the ALD process and will arrive at Al_2O_3/Si interface and passivate the dangling bonds partially at the Si surface, which results in the decreased D_{it}. While a higher PDA temperature would result in the deteriorated D_{it} and therefore the deteriorated τ_{eff}. For the flash annealed sample, though there is a high Q_{fix} in the order of 10^{12} cm^{-2}, D_{it} increases to a high value of $\sim 7 \times 10^{12}$ cm^{-2} eV^{-1} which results in the deteriorated τ_{eff}. The results here indicate that D_{it} would determine the passivation performance when it arrives at the order of $\sim 10^{12}$ cm^{-2} eV^{-1} with a high Q_{fix} in the order of 10^{12} cm^{-2}.

The above results indicate that Q_{fix} and D_{it} would interact between each other in terms of passivation performance. To illustrate the relations among Q_{fix}, D_{it} and τ_{eff} more clearly, a series of samples have been prepared to supply more data. A contour map, including Q_{fix}, D_{it} and τ_{eff} is plotted in Fig. 4. The contour map clearly illustrates that both Q_{fix} and D_{it} have a significant impacts on τ_{eff}. The figure of merits would be the high density of Q_{fix} and low density of D_{it} for high passivation performance. High density of D_{it} and low density of Q_{fix} degrade the passivation performance. In addition, high density of Q_{fix} can offset negative effects by the high density of D_{it} on the passivation performance. Fig. 4 also indicates that a density of negative charges in the order of $\sim 10^{12}$ cm^{-2} is not sufficient for an effective field effect passivation. A low density of D_{it} is the prerequisite to get an effective field effect passivation.

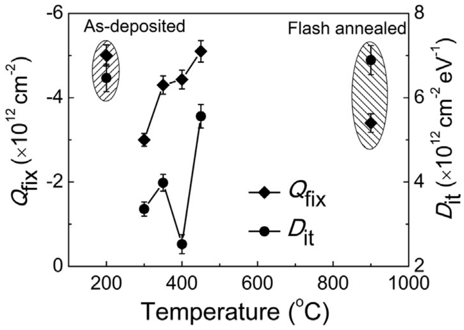

Fig. 3 D_{it} and Q_{fix} of the as-deposited and annealed samples passivated by 30 nm Al_2O_3 films.

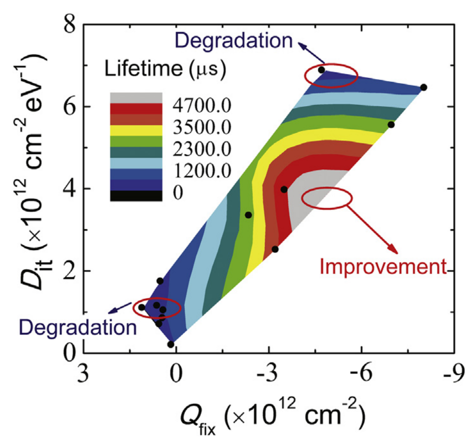

Fig. 4 Contour map of Q_{fix}, D_{it} and minority carrier lifetime (τ_{eff}). Black points show the experimental results.

4. Conclusion

Al_2O_3 layers were deposited by thermal ALD on p-type c-Si wafers. Surface passivation performances were studied as a function of post-deposition annealing conditions. The maximal minority carrier lifetime of ∼4.7 ms was obtained for Al_2O_3 thin films passivated p-type Si. Surface passivation performances of Al_2O_3 films were correlated with negative fixed charges (Q_{fix}) and interfacial state density (D_{it}). The high density of Q_{fix} and low density of D_{it} were needed for high passivation performance, while the high density of D_{it} and low density of Q_{fix} would degrade the passivation performance. A low D_{it} was a prerequisite to benefit from the strong field effect passivation induced by the high density of negative fixed charges in Al_2O_3 films. Interstitial H within Al_2O_3 resulted in the negative fixed charges, while the Si dangling bonds passivated partially by H atoms resulted in the decreased D_{it}, which leaded to the high passivation performances.

Acknowledgments

The authors are grateful for the financial supports from the National Natural Science Foundation of China (No. 11104288) and the Zhejiang Postdoctoral Science Foundation (Bsh1202034).

REFERENCES

[1] T. Dullweber, S. Gatz, H. Hannebauer, T. Falcon, R. Hesse, J. Schmidt, R. Brendel, Prog. Photovolt.: Res. Appl. 20 (2012) 630−638.
[2] S.W. Glunz, Adv. Opt. Electron 2007 (2007). http://dx.doi.org/10.1155/2007/97370. Article ID 97370.
[3] M. Galiazzo, V. Furin, D. Tonini, G. Cellere, A. Baccini, in: Proceeding of the 25th European Photovoltaic Solar Energy Conference, Valencia, Spain, 2010, pp. 2338−2340.
[4] A.G. Aberle, Sol. Energy Mater. Sol. Cells 65 (2001) 239−248.
[5] M.A. Green, Prog. Photovolt.: Res. Appl. 17 (2009) 183−189.
[6] Y. Tsunomura, Y. Yoshimine, M. Taguchi, T. Baba, T. Kinoshita, H. Kanno, H. Sakata, E. Maruyama, M. Tanaka, Sol. Energy Mater. Sol. Cells 93 (2009) 670−673.
[7] I. Martín, M. Vetter, M. Garín, A. Orpella, C. Voz, J. Puigdollers, R. Alcubilla, J. Appl. Phys. 98 (2005) 114912.
[8] B. Hoex, J. Schmidt, P. Pohl, M.C.M. van de Sanden, W.M.M. Kessels, J. Appl. Phys. 104 (2008) 044903.
[9] T. Lüder, B. Raabe, B. Terheiden, in: Proceeding of the 25th European Photovoltaic Solar Energy Conference, Valencia, Spain, 2010, pp. 2138−2140.
[10] F. Werner, B. Veith, V. Tiba, P. Poodt, F. Roozeboom, R. Brendel, J. Schmidt, Appl. Phys. Lett. 97 (2010) 162103.
[11] L.Q. Zhu, X. Li, Z.H. Yan, H.L. Zhang, Q. Wan, IEEE Electron Dev. Lett. 33 (2012) 1753−1755.
[12] P. Saint-Cast, J. Benick, D. Kania, L. Weiss, M. Hofmann, J. Rentsch, R. Preu, S.W. Glunz, IEEE Electron Dev. Lett. 31 (2010) 695−697.
[13] J. Benick, B. Hoex, M.C.M. van de Sanden, W.M.M. Kessels, O. Schultz, S.W. Glunz, J. Appl. Phys. 92 (2008) 253504.
[14] J. Benick, A. Richter, T.T.A. Li, N.E. Grant, K.R. Mclntosh, Y. Ren, K.J. Weber, M. Hermle, S.W. Glunz, in: 35th IEEE Photovoltaic Specialists Conference (PVSC), 2010, pp. 891−895.
[15] B. Hoex, J.J.H. Gielis, M.C.M. van de Sanden, W.M.M. Kessels, J. Appl. Phys. 104 (2008) 113703.
[16] J.J.H. Gielis, B. Hoex, M.C.M. van de Sanden, W.M.M. Kessels, J. Appl. Phys. 104 (2008) 073701.
[17] B.J. Jones, R.C. Barklie, J. Phys. D-Appl. Phys. 38 (2005) 1178−1181.
[18] R. Antti, A. Teemu, R. Mikko, Langmuir 17 (2001) 6506−6509.
[19] S.M. George, Chem. Rev. 110 (2010) 111−131.
[20] B. Vermang, A. Rothschild, A. Racz, J. John, J. Poortmans, R. Mertens, P. Poodt, V. Tiba, F. Roozeboom, in: Proceeding of the 25th European Photovoltaic Solar Energy Conference, Valencia, Spain, 2010, pp. 1110−1113.
[21] K. Lehovec, A. Slobodskoy, Solid State Electron 7 (1964) 59−79.
[22] P.W. Peacock, J. Robertson, Appl. Phys. Lett. 83 (2003) 2025−2027.